REVIEW ARTICLE

Study of the isothermal bainitic transformation and austenite stability in an advanced Al-rich medium-Mn steel

M. Morawiec[1] · V. Ruiz-Jimenez[2] · C. Garcia-Mateo[2] · J. A. Jimenez[2] · A. Grajcar[3]

Abstract

Isothermal bainitic transformation of a lean medium-Mn steel containing (in mass%) 0.18C–3.6Mn–1.7Al–0.23Si–0.2Mo–0.04–Nb after full austenitization at 1100 °C was studied by means of high resolution dilatometry. The effects of isothermal holding temperatures ranging from 450 to 350 °C on the bainitic transformation kinetics was studied experimentally characterizing the microstructure present after a holding time ranging from 15 min to 2 h. The obtained results showed that the bainitic transformation is uncompleted at temperatures above 425 °C. The carbon enrichment of the austenite during isothermal treatment at 450 °C and 425 °C is not enough to avoid martensitic transformation of the austenite during cooling to room temperature. Thus, it is obtained a mixed structure including bainitic ferrite and martensite. Decreasing the austempering temperature resulted in a more pronounced bainite formation. The kinetics of the transformation during austempering at 350 °C is quite similar to that observed at 400 °C, so that 60 min are needed in both cases to complete the reaction. However, local variations in chemical composition associated to segregation of Mn and Al during casting solidification results in differences in the transformation rate of bainitic reaction between different areas in the material. A balance difference between the dendritic and interdendritic areas is responsible for the differences observed among test samples in the kinetics of the isothermal bainitic transformation and the final microstructure.

Keywords Hot-rolled sheet · Dilatometry study · Retained austenite · Phase transformation kinetic · Bainite formation

1 Introduction

Development of medium manganese steels containing from 3 to 12% of Mn [1] has attracted growing interest over the last years [2] in the automotive industry due to their good combination of strength, ductility and sheet formability [3]. Moreover, they offer the possibility for further mechanical properties enhancement by the development of ultra-fine complex microstructures containing a high fraction of retained austenite, which can transform to martensite during deformation at room temperature (TRIP effect) [1]. The thermal and mechanical stability of retained austenite is mainly determined by its C and Mn content [4], but it is also affected by other microstructural factors such as grain size [3], dislocation density and morphology [5]. All these factors are highly dependent upon the heat treatment parameters and/or the processing steps.

Different heat treatment strategies have been developed for the production of medium-Mn sheet steels. The most widely processing schedule used to stabilize a high fraction of retained austenite at room temperature with the optimal stability comprises intercritical annealing after cold rolling [6]. The cold deformation increases the initial energy of material (mechanical energy), leading to faster formation of austenite [7]. During this treatment, the partitioning of carbon [8] and manganese from ferrite to the austenite takes place. As C content has major influence on austenite mechanical behavior [9], some authors have designed a treatment scheme including a two-step intercritical annealing [10] to further increase the carbon enrichment [11].

✉ A. Grajcar
adam.grajcar@polsl.pl

1 Faculty of Mechanical Engineering, Materials Research Laboratory, Silesian University of Technology, 18a Konarskiego Street, 44-100 Gliwice, Poland

2 National Center for Metallurgical Research, Av. de Gregorio del Amo, 8, 28040 Madrid, Spain

3 Faculty of Mechanical Engineering, Department of Engineering Materials and Biomaterials, Silesian University of Technology, 18a Konarskiego Street, 44-100 Gliwice, Poland

However, much less attention has been paid to eliminate the cold rolling step, stabilizing retained austenite in hot-rolled flat products of medium-Mn steels. The hot-rolled sheets can behave during the heat treatment in a different way compared to the cold-rolled products due to differences in the initial microstructure of austenite produced during austenitization [12]. Some works have shown problems with the use of hot rolling followed by slow cooling in the intercritical transformation region [13]. The major difficulty is a lack of ferrite formation even during very slow cooling from the austenite region [14].

A more typical approach of replacing cold rolling and intercritical annealing consists of the isothermal holding after hot rolling of steel in the bainite formation region [15]. This holding temperature corresponds to sheet steel coiling temperature in the industrial production of medium-Mn steels. As bainite keeps in solid solution much lower amount of carbon than the austenite [16], the carbon partitioning during the bainite transformation will stabilize the remaining austenite when carbide precipitation can be suppressed. The typical approach to prevent carbide formation during the bainitic transformation is to use higher Si/Al contents [17]. There are some advantages and disadvantages with the use of these elements. Silicon doesn't decrease the strength of steel but deteriorates the wettability of sheet surface by liquid zinc during dip hot galvanizing [18]. In case of aluminum, although it doesn't influence the wettability [19] it decreases both the density and the strength of steel [20].

It is well known that Mn is an austenite stabilizer, and therefore it reduces the activity of carbon in austenite and retards the austenite decomposition [14]. Guo et al. [21] have found that the incubation and completion time of the isothermal bainitic transformation can be almost doubled by increasing the amount of Mn from 0.43 to 1 mass %. Liu et al. [22] have also reported that additions of Mn or Si and Mn to Fe-Ti-C alloys decrease the activity of carbon in austenite and retard the bainite transformation. Changle et al. [23] have analyzed the effect of Mn content on the bainitic reaction kinetics, retained austenite carbon enrichment and mechanical properties. They reported that as the manganese content increases, the bainitic transformation C-curve moves to longer times, the transformation start temperature decreases and the carbon content of retained austenite is lowered.

To obtain superior strength-ductility balance in medium-Mn steels, the presence of a final amount of retained austenite stabilized at room temperature with a proper balance between Mn and C is critical. This task still is a challenge that requires the understanding of the influence of all alloying elements in the retained austenite stabilization. Beside the chemical composition, it is crucial to optimize the manufacturing parameters including austenitizing condition and the isothermal holding temperature and time for the bainitic

transformation. This work is focused on the analysis of the effects of isothermal holding temperature and time on the bainite transformation kinetics and retained austenite stability of a lean medium-Mn steel containing 0.18% C and 3.6% Mn.

2 Material and methods

2.1 Material

An Al-rich medium-Mn steel with the composition (in mass%) 0.18C–3.6Mn–1.7Al–0.23Si–0.2Mo–0.04Nb was induction melted in a vacuum induction furnace under Ar atmosphere and cast to an ingot into a cylindrical mold of 124 mm internal diameter and 200 mm high. This ingot was forged in the temperature range between 1200 and 900 °C to obtain a strip with final dimension of about 160 mm width and 22 mm thickness. To supress carbide formation during the bainitic transformation, the alloy contains 1.7%Al to avoid the negative effect of Si on sheet wettability. The steel was also microalloyed with 0.2% Mo and 0.04%Nb to refine the microstructure (prior austenite grains as well as retained austenite and bainite laths) and to increase the yield strength due to precipitation strengthening of NbC and refinement of bainite lath structure [24].

2.2 Dilatometry study

A first set of dilatometric measurements was performed to obtain the critical transformation temperatures Ac_1, Ac_3 and M_s according to the ASTM A1033-04 standard [25]. The optimal parameters for the austempering treatments were determined from these tests to stabilize retained austenite at room temperature. As shown in Fig. 1, the thermal cycles
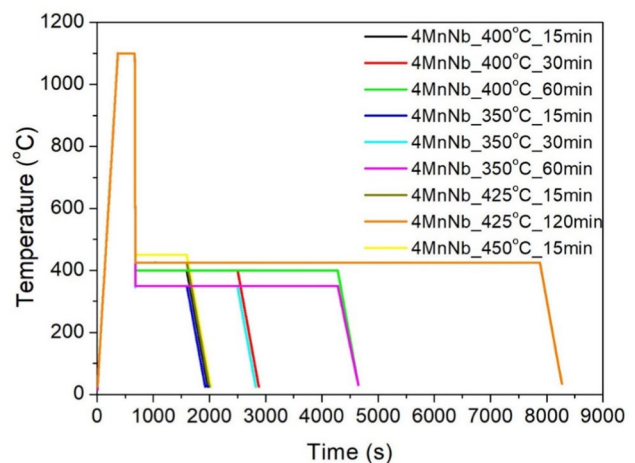

Fig. 1 Heat treatment schedules performed in the dilatometer

started heating from room temperature to 1100 °C at a rate of 3 °Cs^{-1}. After full austenitization at this temperature for 300 s, the samples were cooled down at the rate of 60 °Cs^{-1} to an isothermal holding temperature ranging from 350 to 450 °C, at which the samples were austempered between 15 and 120 min. Finally, the samples were cooled to room temperature at the rate of 1 °Cs^{-1}. All thermal treatments and the study of the kinetics of the bainitic transformation were performed in a BAHR 805A high resolution dilatometer (TA Instruments) under high vacuum conditions using cylindrical specimens of 4 mm diameter and 10 mm length. The longitudinal changes during the tests were measured using a linear variable differential transducer (LVDT) attached to fused silica pushrods with a resolution of ΔL/°C = 0.05 µm/0.05°. The presentation of the dilatation detected during experiments was expressed by the relative change in length (RCL), described by $(\Delta L/L_0)*100\%$. Heating was carried out using an induction coil and cooling was assisted by a blowing helium device. The sample temperature during the thermal cycle was controlled by a K-type thermocouple welded to the sample surface at the center.

2.3 Microstructure characterization

Microstructural evolution after the different isothermal treatments was performed by metallographic examination using light and scanning electron microscope. Specimens for these studies were sectioned and polished following a conventional metallographic technique including standard grinding with abrasive papers up to 2500 grid and a final polish with 1 micron diamond paste. Some polished specimens were etched with a 2% nital (2% nitric acid in ethanol) solution and the revealed microstructure was analyzed with an optical and a scanning electron microscope. Vickers hardness of the different microstructures was measured applying a proof load of 100 N for 15 s.

2.4 Analysis of the retained austenite fraction and carbon content

X-ray diffraction measurements were conducted with Co radiation in a Bruker AXS D8 diffractometer working at 40 kV and 30 mA and equipped with Goebel mirror optics and a LynxEye Linear Position Sensitive Detector. Conventional θ–2θ scans were carried out over a 2θ range of 45–135° with a step size of 0.01°. As austenite may have transformed to martensite due to the metallographic preparation, several etching and polishing cycles were applied to remove the deformed surface layer. The diffraction patterns obtained were refined using the 4.2 version of Rietveld analysis program TOPAS (Bruker AXS) and the crystallographic information of ferrite and austenite for phase quantification as well as for the determination of most important structural

parameters (lattice parameter, crystallite size). For this analysis, the instrumental functions were empirically parameterized using the diffraction pattern of a corundum sample.

3 Results and discussion

3.1 Determination of the critical transformation temperatures

A set of dilatometric measurements using specific heating and cooling rates was performed to locate the transformation temperatures Ac_1, Ac_3 and M_s. Figure 2 shows the relative change in length (RCL) of a dilatometric sample during a thermal cycle consisting of heating from room temperature to 1100 °C at a rate of 3 °Cs^{-1}, holding for 300 s and cooling to room temperature at 60 °Cs^{-1}. On the basis of this figure, the critical temperatures of A_{c1}, A_{c3}, and M_s were determined as 732 °C, 970 °C and 352 °C, respectively. On the other hand, 60 °Cs^{-1} was deemed as sufficient to avoid ferrite/pearlite transformation as only martensitic transformation was detected in the cooling curve.

3.2 Dilatometric analysis and metallographic characterization

3.2.1 Phase transformation kinetics at 450 °C and 425 °C

The dilatation curves at the isothermal holding temperatures of 450 °C and 425 °C and the continuous cooling curves to room temperature after these treatments are shown in Fig. 3a and b, respectively. As it can be observed, after 15 min at 450 °C the relative change in length (RCL) is almost negligible ($\approx 0.02\%$) and the dilatometric response on cooling to room temperature is quite similar to that shown in Fig. 2,
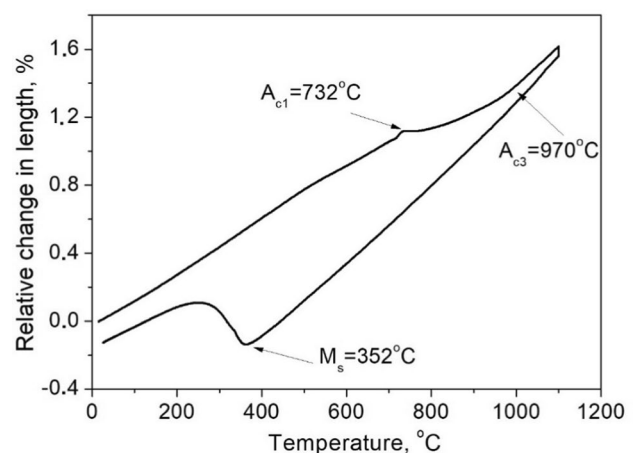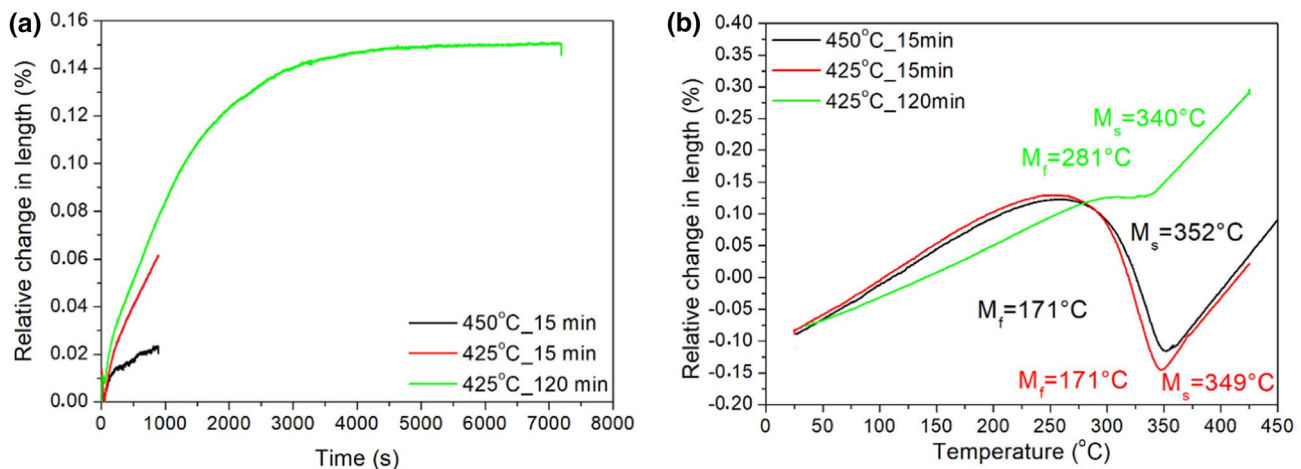

Fig. 2 High-resolution dilatometric curves used to determine the transformation critical temperatures

Fig. 3 Relative change in length **a** during isothermal holding at 450 and 425 °C and **b** during cooling to room temperature after the isothermal holding step

with M_s at 352 °C. It means that neither proeutectoid ferrite nor bainite was formed and hence no carbon enrichment during the isothermal step took place.

Figure 3a shows that decreasing the isothermal holding temperature by 25 °C (425 °C) allows the formation of some bainite. Again, a 15 min treatment only leads to a small increase of the RCL (0.06%), and the dilatometric curve during cooling shown in Fig. 3b is quite similar to that presented for the sample treated 15 min at 450 °C, meaning that almost no bainitic ferrite was formed, probably because the B_s temperature is close to that of the heat treatment. It is necessary to wait about 6000 s at 425 °C to reach a steady state characterized by an approximately constant RLC value, which indicates the end of the bainitic transformation. But the completion of the bainitic transformation at this temperature does not imply a sufficient enrichment of carbon in austenite to avoid martensitic transformation during cooling to room temperature. The most remarkable differences between the cooling curves recorded after 15 min and 120 min at 425 °C is the change in length and the reduction in the slope of the dilatation curve after the martensitic transformation, which means that after 120 min the volume fraction of austenite that transforms to martensite is significantly lower. However, in both cases, the recorded M_s temperature is very similar to the one registered for the bulk chemical composition of the steel ($M_s = 352$ °C), as shown in Fig. 3b. The carbon that leaves the supersaturated ferrite plates can be distributed in austenite in less than tens of seconds. This result would indicate that the carbon content of austenite remains practically constant during the holding treatments.

As the decrease in austenite content after 6000 s at 425 °C is not accompanied by a significant increase in its carbon content, some carbide may precipitate during this treatment in austenite regions with increased carbon content or in the

supersaturated bainitic ferrite. However, as the changes of carbon concentration in austenite caused by the precipitation of bainitic ferrite or carbide favor the formation of other carbides or ferrite, it results very difficult to determine which phase (ferrite or austenite) has been the carbon supersaturated matrix of the carbide precipitation.

The presence of bainitic ferrite after isothermal holding at 425 °C was confirmed metallographically. As shown in the SEM micrographs of Fig. 4, samples treated for 15 min and 120 min present a microstructure mainly composed of bainitic ferrite and martensite. In line with the dilatometric results, the comparison between both micrographs, allowed to conclude that the amount of bainitic ferrite increases with the holding time.

3.2.2 Phase transformation kinetics at 400 °C

Decreasing the isothermal holding temperature to 400 °C resulted in a more pronounced bainite formation, as shown in Fig. 5. According to Fig. 5a, the bainitic transformation reached a steady state, characterized by a relative change in length of about 0.35%, after 60 min holding at this temperature. As expected, the transformation becomes slower when decreasing the transformation temperature, and an incubation time of about 100 s is measured before the transformation starts. In this particular treatment it is detected that the relative change in length, Fig. 5a, for the three holdings do not overlap. This could be associated with local variations on chemical composition due to segregation of Mn and Al during casting solidification [26] and to the position in the forged material from which the dilatometer sample was machined. The presence of a banded microstructure in as forged material indicates the presence of chemical segregation. On the other hand, Grajcar et al. [27] have confirmed
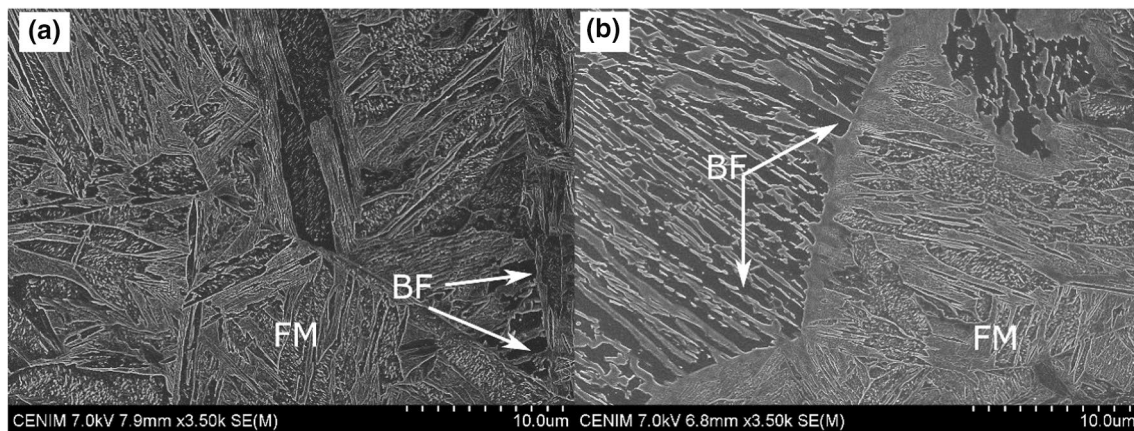
Fig. 4 SEM micrographs after isothermal holding at 425 °C for **a** 15 min and **b** 120 min. *BF* bainitic ferrite, *FM* fresh martensite
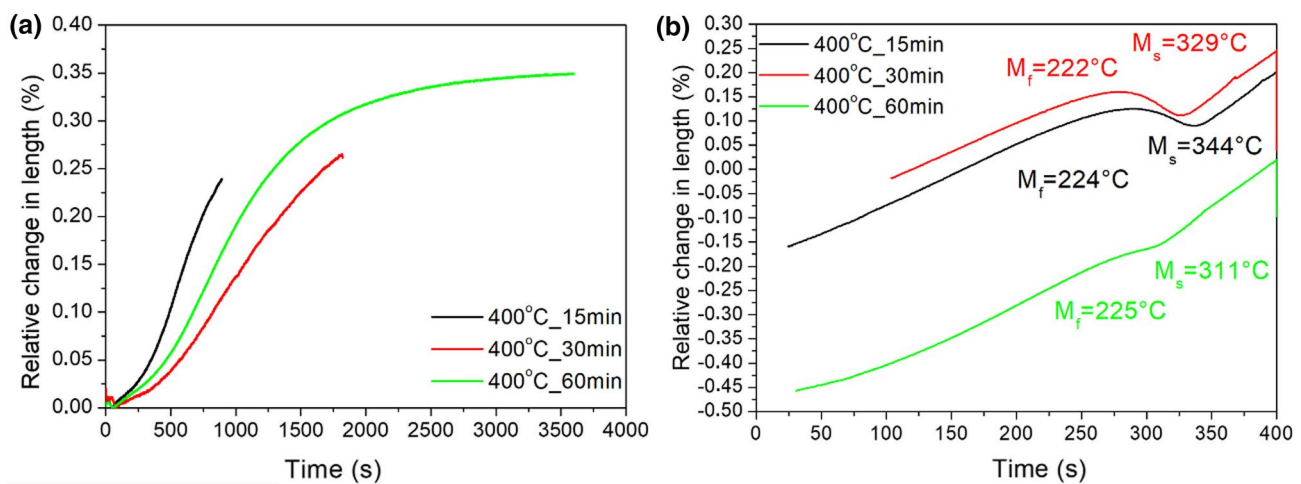
Fig. 5 Relative change in length **a** during isothermal holding at 400 °C and **b** during cooling to room temperature after the isothermal holding step at this temperature

that in a steel with the same chemical composition but a slightly lower manganese content (3.1% instead 3.6%), the Al and Mn contents may differ up to 1 and 1.8 wt.%, respectively. Both elements, Mn and Al have opposite effects on the M_s temperature and the bainite transformation kinetics. On the one hand, Al as an α-forming element accelerates the bainite formation [28] and slightly increases the M_s temperature [29]. On the other hand, Mn as γ-forming element slows down the bainite formation rate [21] and decreases the martensite start temperature [30].

In addition to this effect, it has to be considered that during austempering, these alloying elements are almost immobile relative to iron, but carbon can diffuse at an appreciable rate. Carbon diffusion will control the kinetics of the bainitic reaction, but as Mn reduces the C activity [31], the areas with higher Mn concentration formed by segregation of this element during solidification will be enriched in C

with increasing annealing time, giving place to an inhomogeneous distribution of C in the austenite. As a result, C concentration on the dendritic areas with lower Mn content is lower than in the interdendritic areas with higher Mn, which means different rate of bainitic reaction in both zones. The bainitic transformation will start in the dendritic areas, which have higher transformation temperature and transformation rate. In the interdendritic areas with the highest Mn concentration, the transformation temperature is lower and the transformation rate is slow.

This is in line with previous results, as reported by Changle et al. [23], the higher the manganese content in steel, the lower is the carbon enrichment of retained austenite. Similar result was reported by De Moor et al. [32], who analyzed the correlation between C and Mn contents in steel containing 5.7% Mn. According to their study manganese replaces carbon in austenite, especially at lower temperatures

(below 600 °C). Moreover, Changle et al. [23] also reported that during the bainite transformation the carbon content in the untransformed austenite increases because of C redistribution. This phenomenon results in formation of carbon-rich and carbon-depleted regions in austenite.

Thus, different locations of test samples in the cast material can cause the balance between the dendritic and interdendritic volume fraction to vary from sample to sample, and consequently the average kinetics of the isothermal bainitic transformation. This balance difference between the dendritic and interdendritic areas is also responsible for the lack of correlation between the initial values for the relative change in length with the holding times used for the isothermal treatment observed in Fig. 5b. This figure shows also a decrease in the M_s temperature and the amount of austenite that is transformed into martensite during cooling as the transformation progresses, associated with an increase in the C content in solid solution and therefore its thermal stability. After holding for 60 min, the higher amount of transformed bainite and the migration of excess carbon from the transformed areas to the adjacent non-transformed austenite, cause a considerable decrease in the amount of new martensite formed during cooling and in the M_s until 311 °C.

The microstructure of the steel cooled to room temperature after austempering at 400 °C contained different amount of bainitic ferrite, martensite and retained austenite depending on the holding time, as shown in Fig. 6. As observed in this figure, bainitic ferrite mainly appears as thin units aligned parallel with each other with films of retained austenite between them. Austenite was also found together with martensite in MA islands, which present an internal structure formed by very small martensite laths, surrounded by retained austenite blocks. During austempering, the areas with higher Mn concentration will be enriched in C with increasing annealing time, decreasing the bainite start temperature B_s in the interdendritic areas. The presence of martensite-austenite islands would indicate that the bainitic reaction was incomplete in these Mn and C-enriched areas, and thus the remaining austenite may be partially transformed into martensite during the final quench after the isothermal treatment.

3.2.3 Phase transformation kinetics at 350 °C

The phase obtained from the isothermal decomposition of austenite below M_s can be purely bainitic, purely martensitic or a mix of lower bainite, martensite and some blocks of tempered martensite including carbide precipitation. The formation of isothermal martensite has mainly been observed in high alloy steels with a low Ms temperature, high-carbon steels and Fe–Ni alloys with up to about 25% Ni [33]. In hypoeutectoid steels, the plates of martensite would stop growing very quick once a holding temperature below
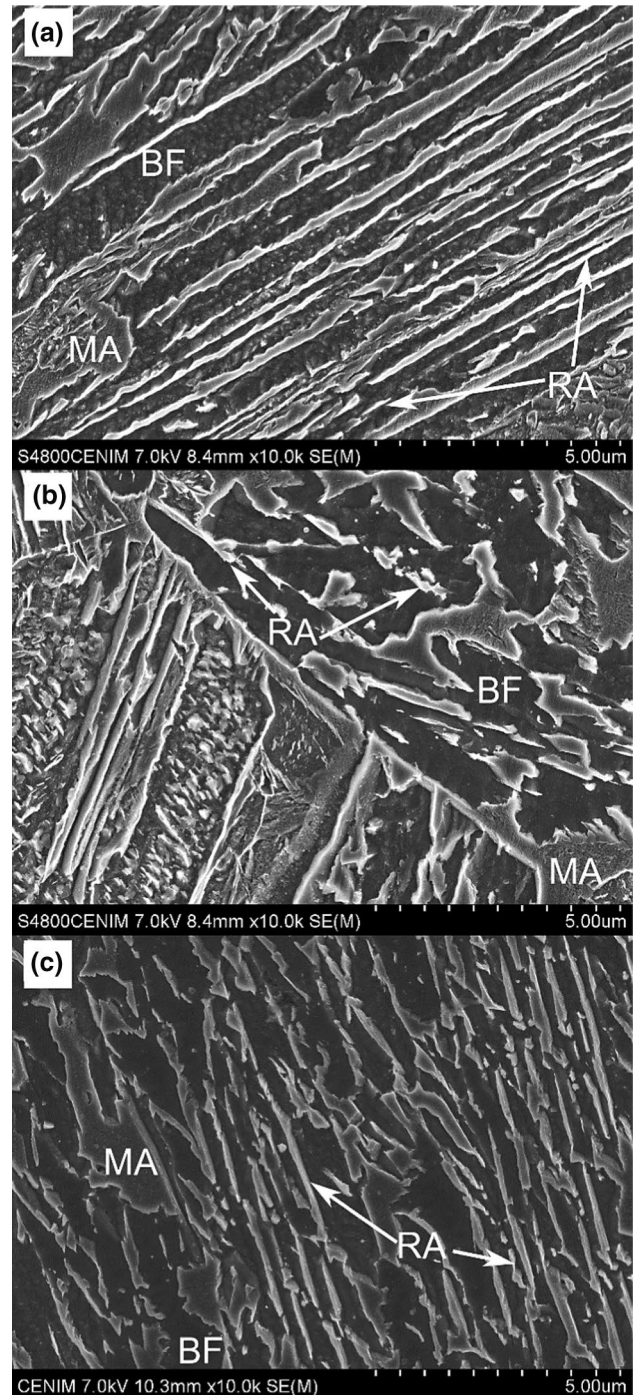
Fig. 6 SEM micrographs after isothermal holding at 400 °C for **a** 15 min, **b** 30 min, **c** 60 min; *BF* bainitic ferrite, *MA* martensitic-austenitic islands, *RA* retained austenite

the M_s is reached due to the high growth rate of martensite (of the order of 1000 m/s). Thus, Navarro-López et al. [34] have reported that in a steel containing 0.2 wt% C, bainitic ferrite is the isothermal product formed in treatments below M_s, where prior athermal martensite had already formed. As our steel contains 0.18 wt% C, it was concluded that the

relative change of length recorded during isothermal holding at 350 °C is basically associated to the volume expansion caused by the bainitic transformation.

The kinetics of the transformation during austempering at 350 °C shows that, as in the case of the 400 °C treatment, the transformation is already finished after 60 min of holding. In this particular case, it seems that the completion of the transformation is reached in between 30 and 60 min. Due to the slower diffusion rate of carbon, a longer incubation time is typically required for the transformation at lower temperatures. However, it has been suggested in the previous study [34] that the martensite/austenite interfaces act as potential nucleation sites. Thus, the existence of athermal martensite prior to the bainitic transformation could accelerate strongly the formation of bainitic ferrite. Furthemore, as the volume increase associated with the formation of some martensite during cooling to the isothermal transformation temperature causes deformation of the adjacent substance, there is a decrease in the incubation time required for the bainitic reaction. As a result of all these factors, the onset of the bainite transformation occurs much faster.

The absence of an incubation time in the RLC curves shown in Fig. 7a would seem to indicate that the transformation begins immediately after achieving the treatment temperature of 350 °C. However, the incubation time of the bainitic reaction cannot be rigorously evaluated from these expansion curves due to the differences in transformation rates between different areas in the steel and the type of microstructure formed in them. In the determination of the M_s from the cooling curves it is not taken into account segregations, so in practice the critical M_s temperatures of 352 °C determined from Fig. 2 correspond to an average value for the alloy concentration in the steel. But due to segregations (Fig. 8), there are differences in transformation behavior between different areas and a deviation from the expected linear dependence starts to be observed at around 415 °C, as it is shown in Fig. 7c. According to Bohemen [35], the deviation from the linear tendency could be the result not from phase transformation, but rather the slower BCC phase lattice contraction during cooling. According to the research, bellow 700 K, a change of length slowly deviates from the linear nature. When the temperature of 600 K is crossed, the deviation is stronger. The effect is higher with closing the material the absolute zero temperature.

However, the characteristic segregation bands (marked by red dashed lines) are visible using light (Fig. 8a, c) and scanning electron microscopy (Fig. 8b, d). The lines of martensite (M) between bainitic ferrite (BF) are the result of local chemical composition differences leading to different austenite stability. According to the EDS measurements of the steel after heat treatment (Fig. 9), there is some deviation of Mn and Al elements in the microstructure. The differences between highest and lowest manganese and aluminum
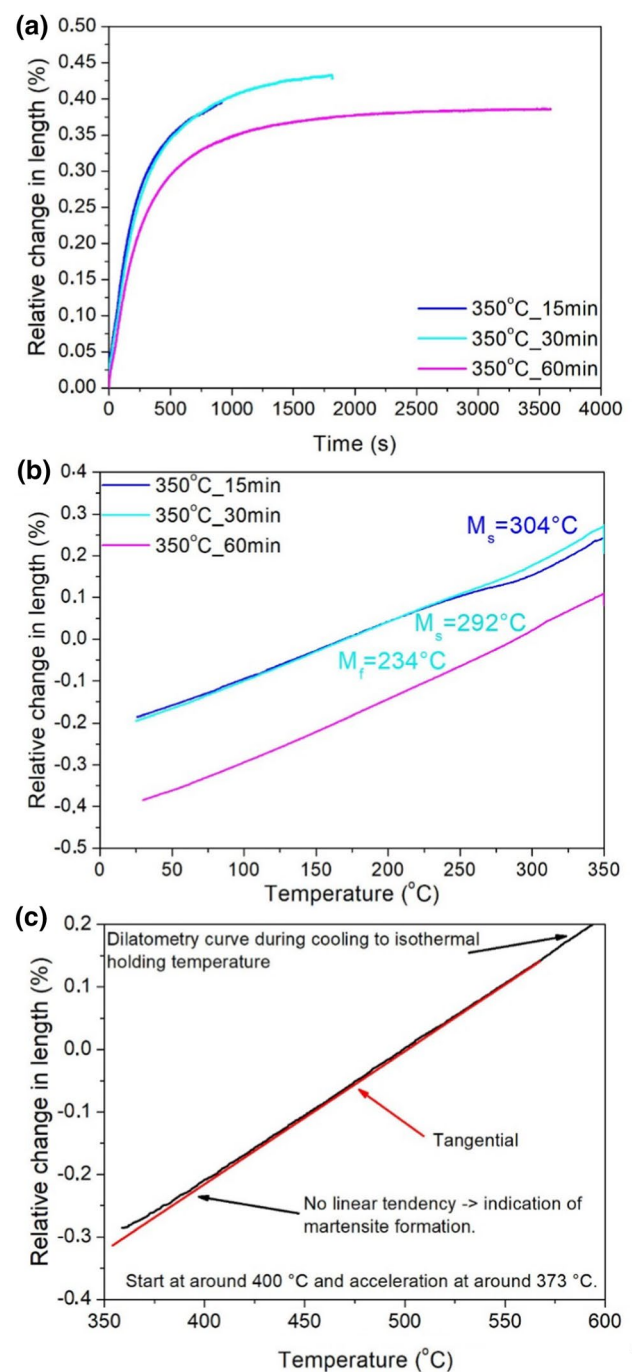

Fig. 7 Relative change in length **a** during isothermal holding at 350 °C and **b** during cooling to room temperature after the isothermal holding step at this temperature **c** during cooling to isothermal holding temperature

contents were 1.2 and 0.5%, respectively. Using the registered EDS results, the M_s temperature at each measurement point was calculated. According to it, the difference between the maximum (323 °C) and minimum (276 °C) martensite start temperature is equal to 47 °C. On the one hand the martensite is more prone to form in the area of higher Mn
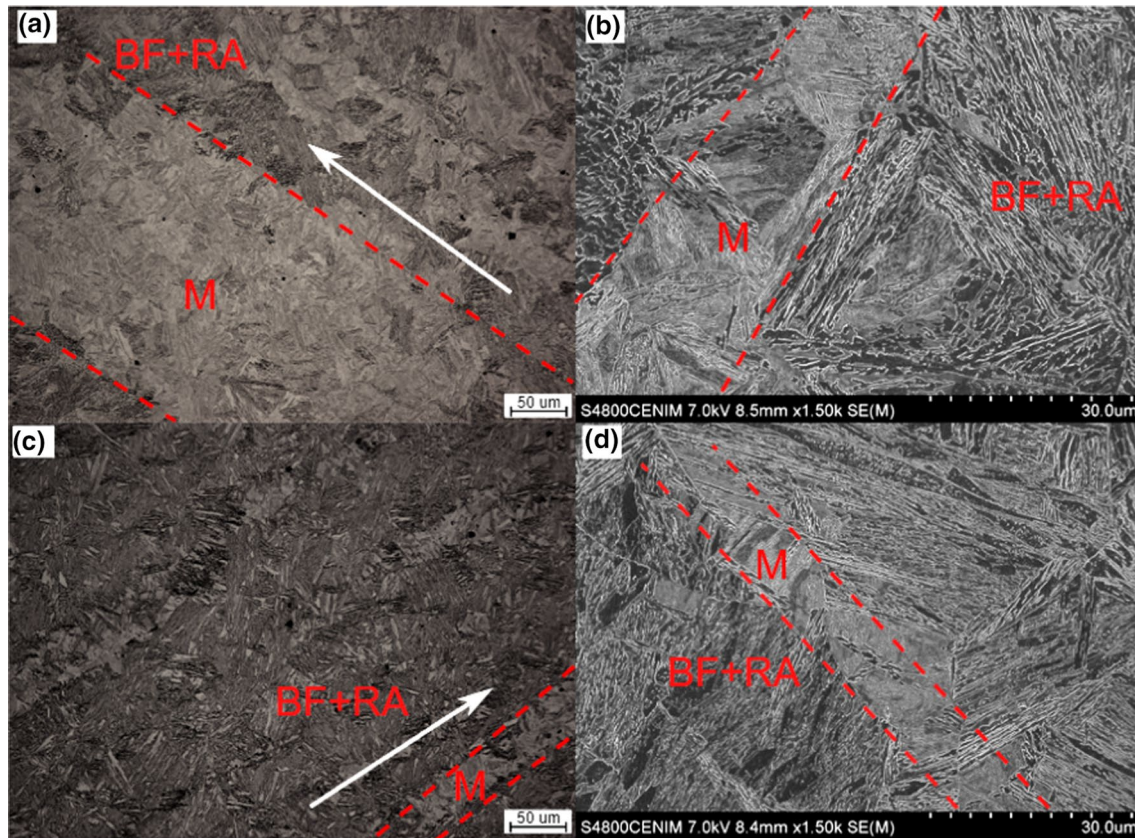
Fig. 8 Segregation bands in the microstructure after heat treatment: **a**, **b** at 400 °C, **c**, **d** at 350 °C, isothermally treated for 15 min. *M* martensite, *BF* bainitic ferrite, *RA* retained austenite
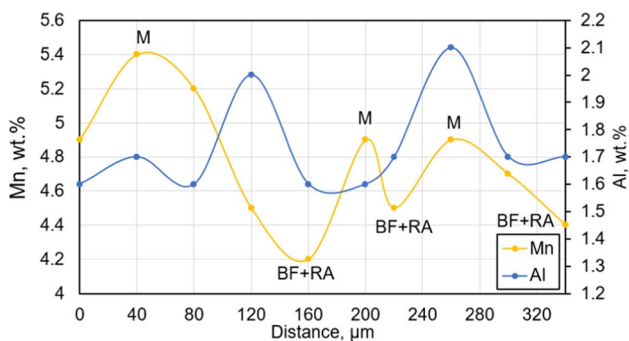
Fig. 9 EDS measurements of manganese and aluminum contents in the microstructure after heat treatment. The distance between points was 40 μm; Sample: treated at 400 °C for 15 min

enrichment (Mn delays the bainitic transformation). On the other hand, areas with lower Mn and higher Al concentrations are subjected to bainitic ferrite formation because such chemical composition accelerates the bainite transformation kinetics. The newly formed bainite enriches the austenite in carbon increasing its stability. Hence, the γ phase with high-carbon content remains stable as retained austenite RA. The areas of higher Mn content and less enriched in

carbon transform into fresh martensite upon final cooling. The width of martensite bands is between 40 and 150 μm.

This deviation would indicate that some martensite can be formed in the Mn depleted regions during cooling, previously to the holding treatment at 350 °C. In these regions, the existence of athermal martensite prior to the bainitic transformation would accelerate strongly the formation of bainitic ferrite [34] since as previous studies suggest, the martensite/austenite interfaces act as potential nucleation sites [36]. On the other hand, the shape strain caused by the formation of martensite before the bainitic reaction [37] would be accommodated by the plastic deformation of the adjacent austenite, leading to a further increase of preferable places for the formation of bainite [38]. As a result of all these factors, the RCL dilatometric curves of Fig. 7a seem to reach the plateau earlier than the RCL curves of Fig. 5a.

The partial transformation to martensite of the areas with the lowest Mn concentration during cooling to 350 °C makes the dispersion in the kinetics of the isothermal bainitic transformation among different test samples observed in Fig. 7a lower than that observed in Fig. 5a for the samples austempered at 400°C. The formation of martensite previous to the isothermal treatment should leave less austenite

for the subsequent bainitic transformation, and therefore to less C enrichment in the austenite. But comparing Figs. 5b and 7b corresponding to holding treatments at 400 °C and 350 °C, respectively, it is clear that the stability of austenite is enhanced by lowering the treatment temperature and/or increasing the holding time. For the treatment at 350 °C, Fig. 7b shows some fresh martensite formation after 15 min, while for the 30 min treatment an almost negligible deviation on the RCL curve is detected and none at all for the 60 min case. The austenite can become stable at room temperature by accumulating enough carbon during isothermal holding. An explanation for this behavior is found in the fact that during the isothermal treatment martensite is expected to act as an extra source for austenite C enrichment [39], similar to the case of QP processes [40]. On the other hand, a comparison between Figs. 5a and 7a shows a general increase in the fraction of bainitic ferrite by decreasing the austempering temperature from 400 to 350 °C.

Examples of the microstructure after austempering at 350 °C are shown in Fig. 10. Due to segregations, some differences in the microstructure developed in different areas can be observed during holding at 350 °C and subsequent cooling to room temperature. The transformation may be more advanced in regions with a lower concentration of Mn, with the appearance of bainitic ferrite and intralath carbide precipiates ($\alpha_B + C$) characteristic of a lower bainite (Fig. 10a—wide laths with the intralath carbides). In the areas with a higher Mn content the transformation temperature is lower and the transformation rate is slow. Thus different microstructural constituents can be found in the final microstructure such as lower bainite ($\alpha_B + C$), bainitic ferrite plates (BF), a mixture of interwoven bainitic ferrite and C-enriched retained austenite with lath-like morphology (RA), and islands of fresh martensite and retained austenite (MA/RA). By comparing Figs. 6 and 10, the expected refinement of the microstructure by lowering the transformation temperature can be also observed [41].

3.3 X-ray diffraction analysis

The presence of austenite was detected with acceptable reliability in the X-ray diffraction patterns of the samples austempered at temperatures ranging between 450 to 350 °C. However, this phase could be quantified in stable fits with repeatable output using the Rietveld method only in the samples treated at 400 °C and 350 °C, because in the rest of the samples the volume fraction was limited to approximately 2%. Figure 11 shows the XRD patterns recorded at 400 °C (Fig. 11a) and 350 °C (Fig. 11b). Table 1 lists the results of Rietveld refinement of these XRD patterns and the austenite carbon content calculated from the austenite lattice parameter.
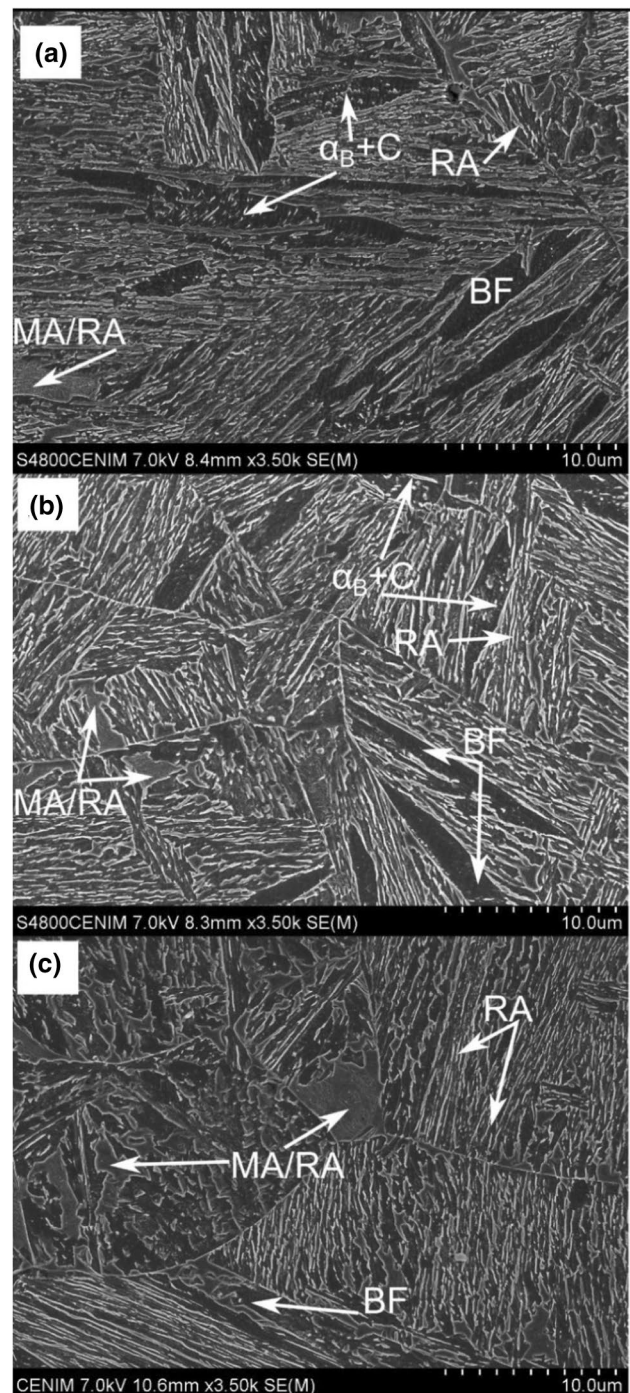
Fig. 10 SEM micrographs after isothermal holding at 350 °C for **a** 15 min, **b** 30 min, **c** 60 min showing lower bainite ($\alpha_B + C$), bainitic ferrite plates (BF), retained austenite (RA), and islands of fresh martensite and retained austenite (MA/RA)

The unit-cell parameter of austenite in Fe–C alloys is defined by the amount of carbon in solid solution. The relationship between both parameters has been extensively studied, but considerable discrepancies can be observed in the values obtained by different investigators. It has been
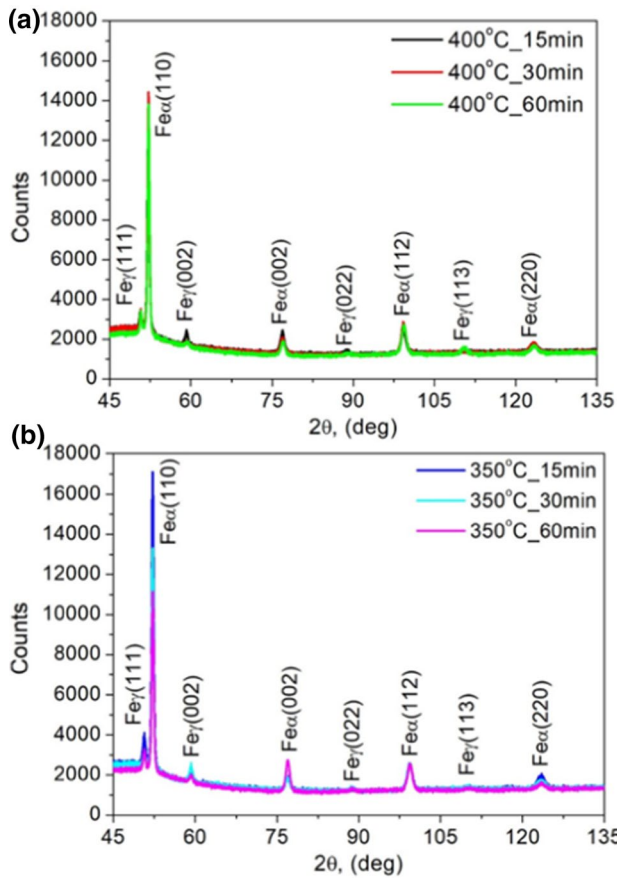
Fig. 11 XRD patterns for the samples subjected to heat treatment at: **a** 400 °C, **b** 350 °C for different times

proposed several relations showing a linear dependence between lattice parameters and atomic or weight percentage of carbon content. An early work of Roberts reported that for a carbon concentration varying from 0.6 to 1.6 mass%, the change in the austenite lattice parameter can be expressed as a function of the C weight percent, x_C, by the relationship (1) [42]:

$$a_\gamma = 3.548 + 0.044x_C \tag{1}$$

However, this expression predicts a value for austenite in pure iron of 3.548 Å, which is significantly smaller than the theoretical value deduced using the relation between the iron atomic radius and the lattice parameters of the austenite ($a_\gamma = 2\sqrt{2}r_{Fe} = 3.564$Å). On the other hand, the extrapolation of the austenite lattice-parameter data obtained at room temperature from Fe–Mn fully austenitic binary alloys to zero % Mn [42], and the extrapolation of the lattice parameter measured for electrolytic iron at high temperature into the austenitic region to room temperature [44] yield to values of 3.570 and 3.576 Å, respectively, for the lattice parameter of pure γ-Fe. Therefore, the dependence of lattice parameter on carbon content should be driven combining this value with a linear dependence with the carbon content, as reported by Cheng et al. (2) [45]:

$$a_\gamma = 3.573 + 0.0070x_C^r \tag{2}$$

where x_C^r is the number of carbon atoms per 100 iron atoms.

It has been reported that Al and Mn expand the austenite lattice because of their larger size compared with iron atom, while Si has a negligible influence. Although both elements expand linearly the austenitic lattice with composition, the effect of aluminum is about one order of magnitude bigger than manganese. Lehnhoff et al. [46] have been reported that 2.5 mass% Al alloying increases the austenite lattice parameter by 1.41×10^{-3} nm. Combining these results with the linear relationship characterizing the increase in austenite lattice parameter with the at% of Mn reported by Marinelli et al. [43], it is obtained the following expression (3) for the dependence of lattice parameter on carbon content for this alloy:

$$a_\gamma = 3.5845 + 0.0070x_C^r \tag{3}$$

The analysis of the evolution of the retained austenite fraction and its carbon content with the austempering

Table 1 XRD results for all variants of heat treatment

Isothermal temperature [°C]	Holding time [min]	Retained austenite (mass %)	Lattice parameter (Å) ±0.02	Austenite C content (mass%) ±0.06
450	15	≤2	–	
425	15	≤2	–	
	120	≤3	–	
400	15	11±2	3.620	1.13
	30	13±2	3.616	1.00
	60	12±2	3.614	0.94
350	15	13±2	3.621	1.16
	30	12±2	3.620	1.13
	60	12±2	3.618	1.07

temperature and holding time is not obvious. The volume fraction of retained austenite depends significantly on the isothermal transformation temperature and time, but the values reported in Table 1 do not show a clear dependence with these parameters. The differences between the values of the austenite lattice parameter shown in Table 1 among the different samples are very small, and of the order of error in the measurements for some samples. During the heat treatments, the carbon diffuses according to its activity gradient, making the areas with the lowest content of Mn to become depleted in carbon. Part of the austenite characterized by a lower content of C can transform into martensite during cooling to room temperature, making the non-transformed austenite correspond mostly to that stabilized by a higher carbon content, and then the information obtained from XRD patterns corresponds only to the austenite present in the areas with high Mn concentration. It is not possible from these XRD patterns to determine the actual austenite content before cooling the samples to room temperature, since the reflections of the ferritic phase include the contribution of both, bainitic ferrite and fresh martensite. Furthermore, the inhomogeneous distribution of C in austenite during the isothermal treatments associated with Mn segregation will determine a different amount of retained austenite in the dendritic and interdendritic areas. As the balance between the dendritic and interdendritic volume fraction may depend on the locations of test samples in the cast material, the result is that the retained austenite fraction may vary from sample to sample even though the treatment conditions are the same. In situ diffraction measurements during the bainitic transformation using synchrotron radiation or a neutron source should be performed to determine the evolution both the true mean C content in the austenite and the fraction of this phase present in the microstructure.

Although the results shown in Table 1 are associated with a high standard dispersion, they seem to indicate that the fraction of austenite retained after a treatment at 400 °C and 350 °C is almost independent of the duration of the treatment. In the case of the treatment at 350 °C, it can be assumed that when the bainitic transformation is finished, the amount of retained austenite and its carbon content practically coincide with the values measured by XRD. This is because the amount of athermic martensite formed before the isothermal treatment is very low since this temperature is only 2 °C lower than the M_s, and besides the curve of cooling to room temperature does not show any martensitic transformation. But as the Fig. 5b shows, after holding at 400 °C some amount of martensite is always formed on cooling to room temperatures. The actual amount of austenite has to be obtained by computing both contribution, and then the mean C content of austenite at such T can determined keeping in mind that

$$(C\gamma * f\gamma)_{\text{Iso}} = (C\gamma * f\gamma)_{\text{RT}} + (C\alpha' * f\alpha')_{\text{RT}} \quad (4)$$

and

$$(f\gamma)_{\text{Iso}} = (f\gamma)_{\text{RT}} + (f\alpha')_{\text{RT}} \quad (5)$$

and

$$C\alpha'_{\text{RT}} = C\text{Bulk} - ((C\gamma * f\gamma)_{\text{RT}+} + (C\alpha * f\alpha)_{\text{RT}})/f\alpha'_{\text{RT}} \quad (6)$$

where $C\alpha = 0.03$ mass.% [47].

Considering that Table 1 shows that the $(f\gamma)_{\text{RT}}$ and $(C\gamma)_{\text{RT}}$ are almost independent on the holding time at 400 °C, the decrease in the amount of martensite formed during cooling as the baintic transformation progresses will be accompanied by a decrease in the actual amount of austenite present, and its C carbon has to increase to satisfy the previous expressions, in line with the discussed dilatometric results. Within the uncertainties of the results, it is possible to conclude that indeed lowering the transformation temperature lead to higher fractions of bainitic ferrite and more C-enriched austenite, in line with the dilatometry observations.

Having retained austenite fractions calculated from the XRD patterns, it is possible to determine the total bainite and fresh martensite amount in the microstructure by completing the rest of the phases included in the microstructure (bainite and martensite) to 100%. For this goal, we have used the dilatometric curves upon cooling to room temperature to estimate first the amount of fresh martensite. Figure 12 presents the curves registered during cooling to room temperature for all the samples treated at 400 °C, as well as the quenching curve of the steel from the austenitization temperature. The quenching curve was used as reference, and corresponds to a sample including 100% martensite in its microstructure. Comparing the level of the RCL signal corresponding to each isothermal
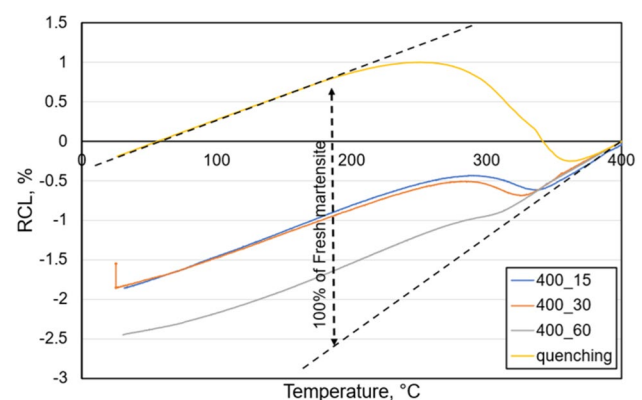
Fig. 12 The example of the way for the determination of fresh martensite fraction, using dilatometric curves during cooling to room temperature after the isothermal holding and quenching

Table 2 The quantitative results of structural constituents determination using XRD (retained austenite) and bainite B and martensite M (dilatometric data)

	RA, %	B + M, %	ΔRCL, %	M, %	B, %
Quenching	0		1.63	100	0
450_15	≤ 2	98	1.63	100	0
425_15	≤ 2	98	1.5	92	6
425_120	≤ 3	97	1.03	63	34
400_15	11 ± 2	89	1.07	66	23
400_30	13 ± 2	87	0.93	57	30
400_60	12 ± 2	88	0.28	17	71
350_15	13 ± 2	87	0.36	22	65
350_30	12 ± 2	88	0.19	12	76
350_60	12 ± 2	88	0.05	3	85
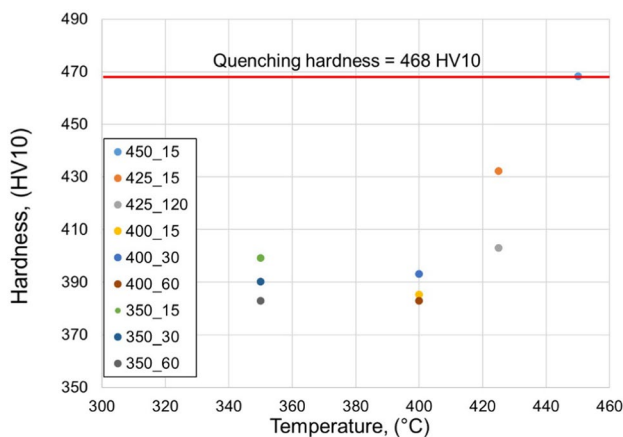
Fig. 13 Hardness measurements for all heat treatment schedules

holding treatment, we can estimate the amount of fresh martensite formed in each case. Then, the amount of bainite is the completion to 100%.

Table 2 shows the result of this quantitative analysis. The ΔRCL was estimated using the RCL from the beginning and finish temperatures of the martensite formation for each curve. According to the presented results, it can be concluded that the prolongation of the isothermal holding time leads to formation of higher amount of bainite. At 400 °C the amount of bainite increases from 23 to 71%, when the isothermal time was increased from 15 to 60 min. At the same time it can be seen that lowering the isothermal temperature results in a higher bainite fraction for the same holding time.

3.4 Hardness

The hardness of this steel decreased as the austempering temperature used decreased. Figure 13 shows the evolution of the hardness with the isothermal temperature and

holding time. Because the isothermal time is too short, after 15 min at 450 °C almost no bainitic ferrite is formed, and the martensite transformation of the austenite during cooling makes that the hardness observed was very similar to the value measured for the sample directly cooled to room temperature at 60 ºC/s after austenitization at 1100 °C. At temperatures below 425 °C, softening occurred due to the isothermal transformation of the austenite into bainitic ferrite. At 425 °C, the bainitic transformation is not completed and the carbon enrichment of the austenite is not enough to avoid martensitic transformation during cooling to room temperature, and thus the mixed structure including bainitic ferrite and martensite makes that the hardness decreased to 430 and 400 HV after 15 min and 120 min holding. Finally, differences on hardness values observed in the samples isothermally treated at 400 °C and 350 °C are quite small, almost independent on the holding time used and ranges from 400 to 380. As the standard uncertainties at hardness value of 400 is about 10 HV, these differences could outcome of the uncertain of the Vickers test. Furthermore, the observed microstructural segregation could also be associated with the dispersion in the observed hardness values.

4 Conclusions

Characteristics of bainitic transformation and the microstructures present in an Al-rich steel containing 3.6Mn and 0.18C (in mass%) are controlled by the holding temperature and time used for this treatment and microsegregation of alloying elements during dendritic solidification:

1. The driving force for bainite formation and the maximum carbon enrichment in the austenite increases as the isothermal holding temperature decreases. Above 425 °C, the bainitic transformation is uncompleted and the carbon enrichment of the austenite is not enough to avoid martensitic transformation of the austenite during cooling to room temperature.
2. Bainitic transformation can be completed at holding temperatures below 400 °C, but a higher fraction of bainitic ferrite is formed at 350 °C than at 400 °C. Since at 350 °C less austenite with higher carbon content is present, this phase can become stable at room temperature and no martensite is formed during cooling to room temperature.
3. Microsegregation of Mn and Al during casting solidification causes different C activity in the dendritic and interdendritic areas resulting in a banded structure. Different tranformation temperatures and transformation rates for both areas make it possible for part of the austenite to transform into martensite before reaching the bulk martensite start temperature.

4. The lack of incubation time in dilatometric curves for samples subjected to isothermal bainitic transformation at 350 °C confirms that the presence of some martensite before the transformation deforms the neighborhood austenite increasing the amount of preferable places for bainite nucleation and the bainite transformation kinetics.

Data availability statement The data that support the findings of this study are available from the corresponding author upon reasonable request.

Declarations

Conflict of interest The authors declare that they have no conflict of interest.

References

1. Kwok TWJ, Rahman KM, Xu X, Bantounas I, Kelleher J, Dasari S, Alam T, Banerjee R, David D. Design of a high strength, high ductility 12 wt% Mn medium manganese steel with hierarchical deformation behavior. Mater Sci Eng A. 2020;782:1–10. https://doi.org/10.1016/j.msea.2020.139258.

2. Yu S, Du LX, Hu J, Misra RDK. Effect of hot rolling temperature on the microstructure and mechanical properties of ultra-low carbon medium manganese steel. Mater Sci Eng A. 2018;731:149–55. https://doi.org/10.1016/j.msea.2018.06.020.

3. Chanden AK, Bansal GK, Kundu J, Chakraborty J, Ghosh-Chowdhury S. Effect of prior austenite grain size on the evolution of microstructure and mechanical properties of an intercritically annealed medium manganese steel. Mater Sci Eng A. 2019;768:1–10. https://doi.org/10.1016/j.msea.2019.138458.

4. Jabłońska MB, Kowalczyk K. Microstructural aspects of energy absorption of high manganese steels. Proc Manuf. 2019;27:91–7. https://doi.org/10.1016/j.promfg.2018.12.049.

5. Lee YK, Han J. Current opinion in medium manganese steel. Mater Sci Technol. 2014;31:843–56. https://doi.org/10.1179/1743284714Y.0000000722.

6. Ding W, Wang R, Li Y, Wang B. High elongation of medium-manganese steel containing 1.0 wt.% Al after a short intercritical annealing time. J Mater Res Technol. 2020;9:7262–72. https://doi.org/10.1016/j.jmrt.2020.04.091.

7. Yan S, Li T, Liang T, Liu X. Adjusting the microstructure evolution, mechanical properties and deformation behaviors of Fe-5.95Mn-1.55Si-1.03Al-0.055C medium Mn steel by cold-rolling reduction ratio. J Mater Res Technol. 2020;9:1314–24. https://doi.org/10.1016/j.jmrt.2019.11.058.

8. Bai Y, Matsui Y, Shibata A, Tsuji N. Effect of thermomechanical processing at α+γ two-phase temperatures on microstructure and mechanical property of 5Mn-0.1C-2Si medium-manganese steel. Mater Sci Eng A. 2019;743:57–66. https://doi.org/10.1016/j.msea.2018.11.061.

9. Haupt M, Dutta A, Ponge D, Sandlobes S, Nellessen M, Hirt G. Influence of intercritcal annealing on microstructure and mechanical properties of a medium manganese steel. Proc Eng. 2017;207:1803–8. https://doi.org/10.1016/j.proeng.2017.10.942.

10. Zhu J, Ding R, He J, Yang ZG, Zhang C, Chen H. A cyclic austenite reversion treatment for stabilizing austenite in the medium manganese steels. Scr Mater. 2017;136:6–10. https://doi.org/10.1016/j.scriptamat.2017.03.038.

11. Xu YB, Hu ZP, Zou Y, Tan DT, Han DT, Chen SQ, Ma DG, Misra RDK. Effect of two-step intercritical annealing on microstructure and mechanical properties of hot-rolled medium manganese TRIP steel containing δ-ferrite. Mater Sci Eng A. 2017;688:40–55. https://doi.org/10.1016/j.msea.2017.01.063.

12. Zhou WH, Wang XL, Venkatasurya PC, Guo H, Shang CJ, Misra RDK. Structure-mechanical property relationship in a high strength low carbon alloy steel processed by two-step intercritical annealing and intercritical tempering. Mater Sci Eng A. 2014;607:569–77. https://doi.org/10.1016/j.msea.2014.03.107.

13. Nakada N, Mizutani K, Tsuchiyama T, Takaki S. Difference in transformation behavior between ferrite and austenite formations in medium manganese steel. Acta Mater. 2014;65:251–8. https://doi.org/10.1016/j.actamat.2013.10.067.

14. Morawiec M, Grajcar A, Zalecki W, Garcia-Mateo C, Opiela M. Dilatometric study of phase transformations in 5 Mn steel subjected to different heat treatments. Materials. 2020;13:1–15. https://doi.org/10.3390/ma13040958.

15. Ravi AM, Kumar A, Herbig M, Sietsma J, Santofimia MJ. Impact of austenite grain boundaries and ferrite nucleation on bainite formation in steels. Acta Mater. 2020;188:424–34. https://doi.org/10.1016/j.actamat.2020.01.065.

16. Yoozbashi MN, Yazdani S, Wang TS. Design of a new nanostructured, high-Si bainitic steel with lower cost production. Mater Des. 2011;32:3248–53. https://doi.org/10.1016/j.matdes.2011.02.031.

17. Pashangeh S, Somani M, Banadkouki SSG. Microstructural evolution in a high-silicon medium carbon steel fallowing quenching and isothermal holding above and below the M_s temperature. J Mater Res Technol. 2020;9:3438–46. https://doi.org/10.1016/j.jmrt.2020.01.081.

18. Grajcar A, Kwasny W, Zalecki W. Microstructure-property relationships in TRIP aided medium-C bainitic steel with lamellar retained austenite. Mater Sci Technol. 2015;31:781–94. https://doi.org/10.1179/1743284714Y.0000000742.

19. Mapelli C, Barella S, Gruttadauria A, Mombelli D, Bizzozero M, Veys X. γ decomposition in Fe–Mn–Al–C lightweight steels. J Mater Res Technol. 2020;9:4604–16. https://doi.org/10.1016/j.jmrt.2020.02.088.

20. Tian J, Xu G, Zhou M, Hu H, Wan X. The effects of Cr and Al addition on transformation and properties in low-carbon bainitic steels. Metals. 2017;40:1–11. https://doi.org/10.3390/met7020040.

21. Guo H, Zhou P, Zhao A, Zhi C, Ding R, Wang JX. Effects of Mn and Cr contents on microstructures and mechanical properties of low temperature bainitic steel. J Iron Steel Res Int. 2017;24:290–5. https://doi.org/10.1016/S1006-706X(17)30042-0.

22. Liu SK, Zhang GY. The effect of Mn and Si on the morphology and kinetics of the bainite transformation in Fe–C–Ti alloys. Metall Trans A. 1990;21:1509–11. https://doi.org/10.1007/BF02672565.

23. Changle Z, Fu H, Shenqqiang M, Yi D, Jian L, Zhenquo X, Yonqping L. Effect of Mn content on microstructure and properties of wear-resistant bainitic steel. Mater Res Express. 2019;6:1–22. https://doi.org/10.1088/2053-1591/ab1c8d.

24. Tarek B, El-Shenawy E, El-Sabbagh A, Taha MA. Feasibility of 00.2% Nb-based microalloyed steel for the application of one-step quenching and partitioning heat treatment. Mater Sci Appl. 2021;12:374–87. https://doi.org/10.4236/msa.2021.128026.

25. ASTM A1033-04; ASTM International: West Conshohocken, (2004). https://www.astm.org/. Accessed 25 Mar 2020

26. Shen Y, Yang S, Liu J, Liu H, Zhang R, Xu H, He Y. Study of micro segregation of high alloy Fe–Mn–C–Al steel. Steel Res Int. 2019. https://doi.org/10.1002/srin.201800546.

27. Grajcar A, Kamińska M, Opiela M, Kalinowska-Ozgowicz E, Skrzypczyk P, Grzegorczyk B. Segregation of alloying elements in thermomechanically rolled medium-Mn multiphase steels. J Achiev Mater Manuf Eng. 2012;55:256–64.

28. Garcia-Mateo C, Caballero FG, Bhadeshia HKDH. Acceleration of low-temperature bainite. ISIJ Int. 2003;43:1821–5. https://doi.org/10.2355/isijinternational.43.1821.

29. Tian J, Xu G, Zhou M, Hu H, Wan X. The effects of Cr and Al addition on transformation and properties in low-carbon bainitic steels. Metals. 2017;7:1–11. https://doi.org/10.3390/met7020040.

30. Farahani H, Xu W, Van der Zwaag S. Predicting the cooperative effect of Mn–Si and Mn–Mo on the incomplete bainite formation in quaternary Fe–C alloys. Phil Mag Lett. 2018;98:161–71. https://doi.org/10.1080/09500839.2018.1515505.

31. Kral L, Million B, Cermak J. Diffusion of carbon and manganese in Fe–C–Mn. Def Diff Forum. 2007;263:153–8. https://doi.org/10.4028/www.scientific.net/DDF.263.153.

32. De Moor E, Matlock DK, Speer JG, Merwin MJ. Austenite stabilization through manganese enrichment. Scr Mater. 2011;64:185–8. https://doi.org/10.1016/j.scriptamat.2010.09.040.

33. Borgenstam A, Hillert M. Activation energy for isothermal martensite in ferrous alloys. Acta Mater. 1997;45:651–62. https://doi.org/10.1016/S1359-6454(96)00186-3.

34. Navarro-Lopez A, Sietsma J, Santofimia MJ. Effect of prior athermal martensite on the isothermal transformation kinetics below M_s in a low-C high-Si steel. Metall Mater Trans A. 2016;47:1028–39. https://doi.org/10.1007/s11661-015-3285-6.

35. Bohemen SMC. The nonlinear lattice expansion of iron alloys in the range 100–1600 K. Scri Mater. 2013;69:315–8. https://doi.org/10.1016/j.scriptamat.2013.05.009.

36. Ravi AM, Navarro-Lopez A, Sietsma J, Santofimia MJ. Influence of martensite/austenite interfaces on bainite formation in low-alloy steels below Ms. Acta Mater. 2020;188:394–405. https://doi.org/10.1016/j.actamat.2020.02.003.

37. Guo H, Feng X, Zhao A, Li Q, Ma J. Influence of prior martensite on bainite transformation, microstructure, and mechanical properties in ultra-fine bainitic steel. Materials. 2019;12:1–15. https://doi.org/10.3390/ma12030527.

38. Smanio V, Sourmail T. Effect of partial martensite transformation on bainite reaction kinetics in different 1%C steels. Solid State Phenom. 2011;172–174:821–6. https://doi.org/10.4028/www.scientific.net/SSP.172-174.821.

39. Hidalgo J, Celada-Casero C, Santofimia MJ. Fracture mechanisms and microstructure in a medium Mn quenching and partitioning steel exhibiting macrosegregation. Mater Sci Eng A. 2019;754:766–77. https://doi.org/10.1016/j.msea.2019.03.055.

40. Toji Y, Miyamoto G, Raabe D. Carbon partitioning during quenching and partitioning heat treatment accompanied by carbide precipitation. Acta Mater. 2015;86:137–47. https://doi.org/10.1016/j.actamat.2014.11.049.

41. Cornide J, Garcia-Mateo C, Capdevila C, Caballero FG. An assessment of the contributing factors to the nanoscale structural refinement of advanced bainitic steels. J Alloys Compd. 2013;577:43–7. https://doi.org/10.1016/j.jallcom.2011.11.066.

42. Roberts CS. Effect of carbon on the volume fraction and lattic parameters of retained austenite and martensite. JOM. 1953;5:203–4. https://doi.org/10.1007/BF03397477.

43. Marinelli P, Buraj A, Guillermet AF, Sade M. Lattice parameters of metastable structures in quenched Fe–Mn alloys. Part I: experimental techniques, bcc and fcc phases. Z Metallkd. 2000;91:957–62.

44. Seki I, Nagata K. Lattice constant of iron and austenite including its supersaturation phase of carbon. ISIJ Int. 2005;45:1789–94. https://doi.org/10.2355/isijinternational.45.1789.

45. Cheng L, Bottger A, Keijser ThH, Mittemeijer EJ. Lattice parameters of iron-carbon and iron–nitrogen martensites and austenites. Scr Met Mater. 1990;24:509–14. https://doi.org/10.1016/0956-716X(90)90192-J.

46. Lehnhoff GR, Findley KO, De Cooman BC. The influence of silicon and aluminum alloying on the lattice parameter and stacking fault energy of austenitic steel. Scrip Mater. 2014;92:19–22. https://doi.org/10.1016/j.scriptamat.2014.07.019.

47. Bhadeshia HKDH, Edmonds DV. Bainite in silicon steels: new composition–property approach Part 1. Met Sci. 1983;17:411–9. https://doi.org/10.1179/030634583790420600.